Stator re-stagger optimization in multistage axial compressor

Propulsion and Power Research 2021;xxx(xxx):1−11

http://ppr.buaa.edu.cn/

Propulsion and Power Research

www.sciencedirect.com

ORIGINAL ARTICLE

Stator re-stagger optimization in multistage axial compressor

Jinguang Yang[a], Min Zhang[a], Cheng Peng[a], Michele Ferlauto[b], Yan Liu[a,*]

[a]*School of Energy and Power, Dalian University of Technology, Dalian, 116024, China*
[b]*Department of Mechanical and Aerospace Engineering, Politecnico di Torino, Turin, 10129, Italy*

Received 24 August 2020; accepted 16 March 2021
Available online XXXX

KEYWORDS

Multistage axial compressor;
Mean-line calculation;
Loss model calibration;
Variable stator vane;
Re-stagger optimization

Abstract As a widely applied technique in multistage axial compressors, variable stator vanes (VSV) can flexibly rematch the blade rows to fulfil a variety of aerodynamic performance requirements, such as high efficiency and wide surge margin. The purpose of this paper is to develop an optimization method to quickly determine VSV settings during the preliminary design phase. A mean-line method with a model calibration procedure is adopted to evaluate compressor performance, and the NSGA-II algorithm is employed for automatic optimization. The developed optimization system is then employed to determined re-stagger arrangement in a multistage compressor. A single-speed optimization with performance constraints of specific operating point and a multi-speed optimization with different control laws are conducted. Results are compared with available experimental re-stagger scheme, which verifies the effectiveness of the re-stagger optimization method. Moreover, method is proposed to determine operating parameters of a working point with a user-defined pressure ratio or mass flow rate after variable geometry.

*Corresponding author.
E-mail address: yanliu@dlut.edu.cn (Yan Liu).

Peer review under responsibility of Beihang University.

Production and Hosting by Elsevier on behalf of KeAi

https://doi.org/10.1016/j.jppr.2021.03.002

Nomenclature

f	objective function
g	constraint condition
i	incidence angle (unit: °)
K	proportionality coefficient
$\dot{m}$	mass flow rate (unit: kg/s)
n	revolution speed (unit: rpm)
N_{row}	blade row number

Greek letters

γ	stagger angle (unit: °)
η	efficiency
η_a	adiabatic efficiency
π_t	total pressure ratio
χ	design variable
ω	total pressure loss

Subscripts

c	constrained operation condition
s	surge condition
ori	original
opt	optimized
ref	reference value

Acronyms

CDA	controlled diffusion airfoil
CP	constrained point
CFD	computational fluid dynamics
DCA	double circular arc
DF	diffusion factor
EMC	empirical model calibration
GA	genetic algorithm
MSOpt	multi-speed re-stagger optimization
SM	surge margin
SSOpt	single-speed re-stagger optimization
SV	stator vane
VSV	variable stator vane

1. Introduction

With the progress of gas turbines and aero engines, requirements such as high-efficiency and high-loading multistage axial compressors are urgent. Meanwhile, the matching problem is also significant since each blade row has its optimum performance at a specific inlet flow angle condition. This condition is termed as design point or match point, which is determined by the design mass flow rate and design revolution ($\dot{m}_d$ and n_d). However, a compressor always encounters off-design conditions, where mass flow ($\dot{m}$) and speed (n) deviate from their design values. As introduced by Aungier [1], at n_d condition, unstable operations referred as surge and choke are commonly occurred when $\dot{m}$ is lower and larger than $\dot{m}_d$ respectively. Meanwhile, front stages often experience stall and then surge, and rear stages are choked when n is lower than n_d. An opposite process will happen when n is higher than n_d [2]. These can induce high aerodynamic loss and even structural damage due to flow oscillation.

In order to avoid stall and subsequent surge operations, various control techniques [3,4] including inter-stage bleeding, multi-spool arrangement, casing treatment and variable stator vanes (VSV) are utilized in multistage axial compressors. Among these performance improvement methods, VSV approach can reduce stage mismatching level and hence satisfy different performance requirements. This technique is also beneficial during engine start-up and acceleration processes [5] or when encountering environmental changes caused by season and flight altitude [6]. It can also be considered in initial design phase of compressors [7], where design condition is generally different from operating condition.

For multistage compressors, variable inlet guide vane (VIGV) or VSV can improve stage matching, as illustrated in Figure 1. Stagger angles of IGV or each stator vane (SV) can be adjusted, and hence inlet flow angles or incidence angles (i) at rotor inlet are changed according to operating conditions. The re-stagger magnitude is often decreased from upstream IGV to downstream SVs [8]. This finally compromises stage mismatching to ensure a wide high-performance operating range and a large surge margin. Therefore, it is necessary to develop a reasonable criterion to determine re-stagger scheme.

In order to determine VSV scheme without using experimental or CFD methods that are highly costly and time-consuming, many researchers have conducted optimization studies using reduced-order models. Roh and Daley [8] optimized re-stagger settings of IGV and SVs of an axial compressor using the particle swarm optimization (PSO) algorithm, where the objective was composed of surge mass flow, polytrophic efficiency and pressure ratio based on a weighting scheme and two speed conditions were considered. Their results indicated that the developed PSO method is an efficient and rapid tool for on-line re-stagger optimization. Regarding a seven-stage aircraft compressor, Sun and Elder [2] carried out a direct research for optimal re-

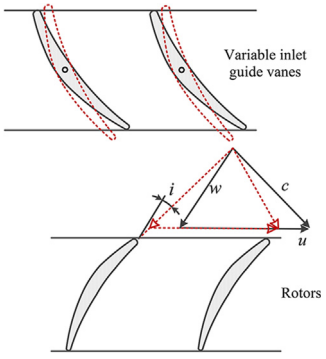

Figure 1 Schematic diagram of re-stagger scheme.

stagger setting based on a sequential weight increasing factor technique (SWIFT). Like the study of Roh and Daley [8], they performed several optimization cases under different single revolution speed, and results also proved that VSV is beneficial to improve performance and realize stage re-matching at part-speed operations. Later, using the same optimization scheme as in Ref. [2], White et al. [9] further demonstrated possibility of VIGV or VSV to improve the compressor performance.

Re-stagger optimization works for VIGV or VSV of Gallar et al. [10] and Reitenbach et al. [11] were conducted from a whole engine cycle point of view. Gallar et al. [10] considered coupled efficiency of compressor and turbine, while Reitenbach et al. [11] integrated engine specific fuel consumption analysis. Both two studies realized appropriate re-stagger schedules that had better surge margin for their compressor. Similarly, Wang et al. [12] numerically evaluated impacts of VSV on the efficiency and fuel consumption of a three-shaft gas turbine. In additions, Li et al. [13] conducted VSV optimization based on artificial neural networks and genetic algorithm. They studied two operating conditions at design-speed and carried out a sensitivity analysis using an established ANN to analyze influence of geometric parameters on compressor performance.

Above-mentioned researches have proved the effectiveness of re-stagger setting to improve the compressor performance. Most of them define multi-objectives in their optimization procedures, however, only a set of operating conditions on one speed line are specified during the optimization process. In addition, one-dimensional (1D) mean-line method combined with proprietary loss models is usually employed for performance calculation. Therefore, prediction accuracy of 1D method is significant for feasibility of optimized VIGV or VSV. This paper does not intend to make comments on accuracy of 1D tools in above studies, but attempt to increase predictive accuracy via a model calibration technique. Based on this, a re-stagger optimization system is developed. Moreover, an optimization considering both single-speed and multiple-speed conditions is conducted. A six-stage axial part of a combined compressor is chosen for re-stagger optimization. The obtained optimized settings are compared with available experimental ones, and verify the correctness of the developed method.

2. Re-stagger optimization method

2.1. Optimization procedure

As already mentioned, the purpose of the re-stagger optimization is to adjust stagger settings of IGV or stator for multistage compressors. The optimization procedure developed in this paper is shown in Figure 2. Key elements include design variables (χ), a performance evaluation solver and an optimization algorithm. The performance indexes are also used in the definition of objective function, i.e., $f(\chi)$. Since χ and $f(\chi)$ are case-dependent considering application requirements and working conditions of a compressor, they will be introduced in detail in Section 4. This section mainly discusses the performance solver and the optimization algorithm.

2.2. One-dimensional mean-line method based on empirical model calibration

Generally, essential performance parameters for compressors contain total pressure ratio (π_t), adiabatic efficiency (η_a) and surge margin (SM). In order to evaluate these variables, a 1D mean-line method is adopted in current study. Calculation stations are located on the mean line of blade rows. With the specified inlet conditions and geometric parameters, compressible fluid relations are employed to solve aerodynamic parameters at the inlet and outlet of each blade row. Different rotational speeds and various operating conditions at a specific speed are considered to get characteristic curves of a compressor.

In order to involve real flow effects, various empirical loss models are integrated in the 1D mean-line analysis code. Empirical models associated with minimum loss

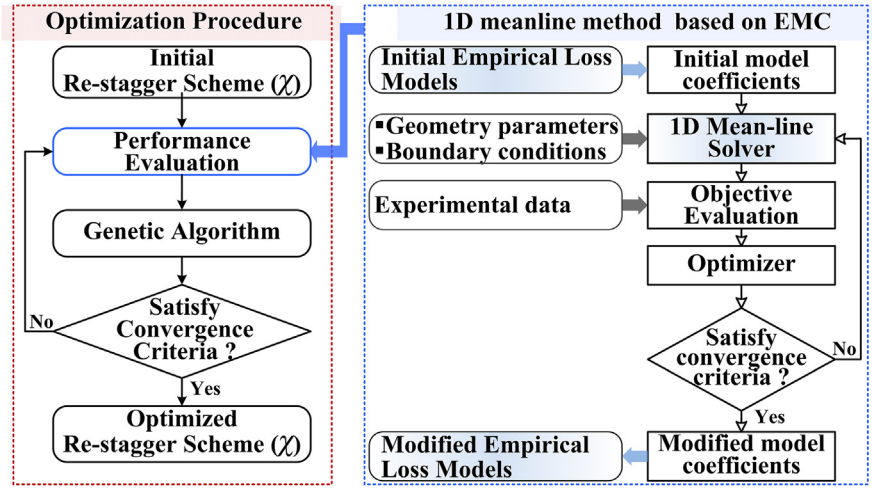

Figure 2 Flow chart of stator re-stagger optimization.

incidence [14], reference deviation [15], off-design deviation [14], profile loss [16], off-design loss [17,18] and end-wall blockage [19] are adopted for the compressor studied in this paper. In addition, since one of main applications of re-stagger setting is to increase SM of multistage compressors, models for estimating stall and surge are also integrated. In the present mean-line code, surge prediction models, such as McKenzie [9], Aungier [1], Koch [20] et al., are included. They can help to determine a relatively reasonable surge boundary line, and hence aid to get an appropriate influence tendency of re-stagger on surge boundary. Mathematical formulations of these empirical loss models are not presented here for the sake of brevity, please refer to the work of Peng [21] for detail.

Empirical loss models can efficiently assess irreversible loss in compressor cascades. However, most of them [22] are established based on early experimental results of some standard cascades, such as NACA-65 series, C series and DCA series. Meanwhile, some models do not take 3D flow effects into account. With development of aerodynamic design techniques, lots of modern blades, such as geometrically parameterized blades and controlled diffusion airfoils, have been widely used in high-performance compressors. Therefore, feasibility and accuracy of existing models needs to be further verified for modern blades with different loading levels and under various working conditions.

Due to the above mentioned issues, an empirical model calibration (EMC) is developed by Peng [21] to improve accuracy of the 1D mean-line solver. The process is presented in the right-hand side of Figure 2. It is also based on an optimization-based scheme, whose design variables are coefficients of empirical models. As a general empirical model system, there are 23 coefficients to be optimized. The objective is to minimize the discrepancy between the performance value predicted by the 1D mean-line solver and that obtained via experiments or 3D CFD predictions. Models associated with minimum loss incidence, deviation and total pressure loss are mainly considered in the calibration process. Meanwhile, the calibration is executed using performance data on the whole characteristic curves of a compressor. This means that loss models are modified to accurately evaluate performance for as more working conditions as possible. During the calibration optimization, the Hausdorff distance is applied to calculate the objective function, and the Nelder-Mead [23] algorithm is adopted to optimize the model coefficients. Feasibility of this 1D mean-line solver based on EMC will be validated in Section 3.2.

It is admitted that calibrated coefficients are case dependent, and this is a natural result. The standard loss and deviation models are aimed to be applied in a general purpose. However their accuracy may be low when applied to a particular application. Since the calibration acts as an improved process of the standard model, it is natural that the calibrated models have a narrower application range compared to the standard ones. So the calibration method is general, but the finally calibrated loss models are case dependent.

2.3. Optimization algorithm

The re-stagger optimization in the current paper is a multi-objective problem, where the objectives will also be discussed thoroughly in Section 4. Therefore, the NSGA-II (non-dominated sorting genetic algorithm II) algorithm [24] is adopted. This algorithm calculates fitness function according to magnitude of objective functions and constraints. Based on fitness function of parent population, selection, crossover, mutation, and recombination operators are executed to generate offspring populations. After multiple generations of screening, solutions termed as Pareto-optimal front are finally obtained. Due to superiorities in simplicity, good robustness and global convergence, the NSGA-II algorithm has been widely applied in engineering and academic fields.

In terms of multiple constraints and objective functions, the non-domination principle is employed here to determine the rank of individuals in parent population. In addition, the crowded-comparison operator is introduced to ensure diversity of population members, and the elite-preserving operator is applied to accelerate convergence of the optimization algorithm.

3. Compressor studied and method validation

3.1. The compressor studied

A P&WA combined compressor [25,26] with VIGV and VSV is selected as the test case. This compressor is designed for a 10 MW class gas turbine. It consists of a six-stage axial compressor and a single-stage centrifugal compressor on the same spool, as shown by the flow-path in Figure 3. In this paper, the re-stagger optimization is applied for the six-stage axial compressor part. Table 1 lists some key performance parameters at the design point.

During experiments in Refs. [25,26], the inlet guide vane and all stators of the P&WA axial compressor are equipped with mechanical devices to reset stagger angles. Varying ranges of re-stagger angles for the IGV and S1−S6 are presented in Table 2 [25]. Meanwhile, Figure 4 shows the experimental re-stagger scheme of the IGV and S1−S2 as a function of revolution. Positive angle value indicates that vane is turned to close, while negative value is just the opposite. For this combined compressor, the purpose of re-stagger is not only to provide an adequate off-design efficiency and surge margin characteristic, but also to achieve flow matching of the axial and centrifugal compressor at part speed. Meanwhile, it is worth mentioning that to satisfy the latter requirement, an inter-stage bleeding technique is adopted in experiments, which is not considered since only axial part is modeled.

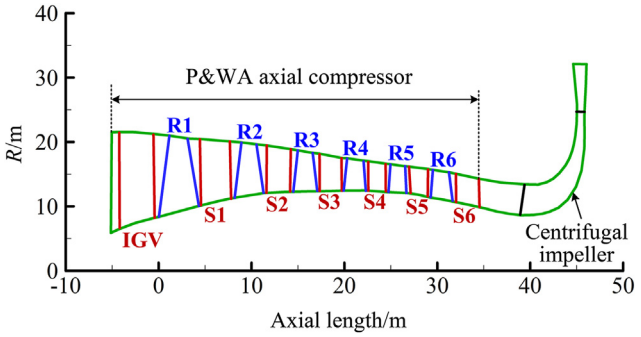

Figure 3 Flow path of the combined compressor.

3.2. Validation of the 1D mean-line solver

In order to validate the 1D method developed in Section 2.2, performance of the P&WA 6-stage compressor is predicted. Coefficients of empirical models are calibrated using the experimental data [25]. It should be mentioned that after a comparison of the three surge estimation models introduced in Section 2.2, the McKenzie model [9] is finally chosen to determine the surge boundary line of the P&WA compressor.

Figure 5 shows the total pressure ratio (π_t) and adiabatic efficiency (η_a) predicted by the 1D solver using the standard and calibrated models respectively. From the comparison results of π_t in Figure 5(a), values predicted by standard models (1D) are higher at all operating conditions, and the 1D calibrated data (1D_C) are nearly consistent with experimental values (EXP). For η_a in Figure 5(b), prediction results using calibrated models are in better agreement with the measured data than those using standard models, except those at speeds of 95%n_d and 50%n_d. Furthermore, predicted mass flow rate at peak efficiency points after calibration are consistent with experimental value. These results prove that the 1D solver with calibrated models can accurately predict the compressor performance. Therefore, the solver and calibrated models can be employed to evaluate objective functions during the re-stagger optimizations.

Table 1 Performance parameters of the P&WA 6-stage.

Parameters	Symbols	Values
Design revolution speed	n_d	15,000 rpm
Design mass flow rate	$\dot{m}_d$	31.572 kg/s
Total pressure ratio	π_t	6.67
Adiabatic efficiency	η_a	89.0%

Table 2 Adjustable ranges of re-stagger settings.

Vane	γ/(°)
IGV	−10, +40
S1	−5, +15
S2	−5, +10
S3	−5, +5
S4	−5, +5
S5	−5, +5
S6	−10, +10

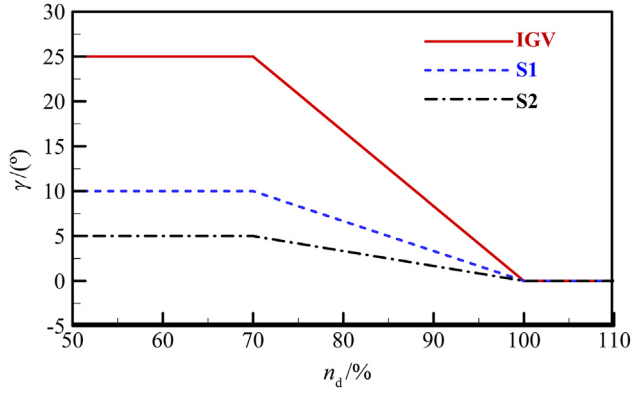

Figure 4 Re-stagger scheme of IGV and S1−S2 in experiments.

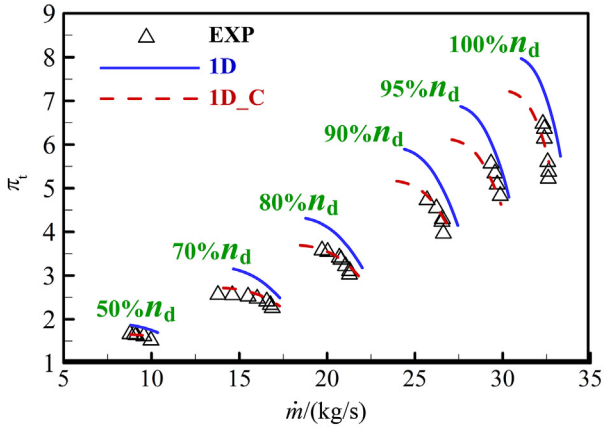

(a) Total pressure ratio

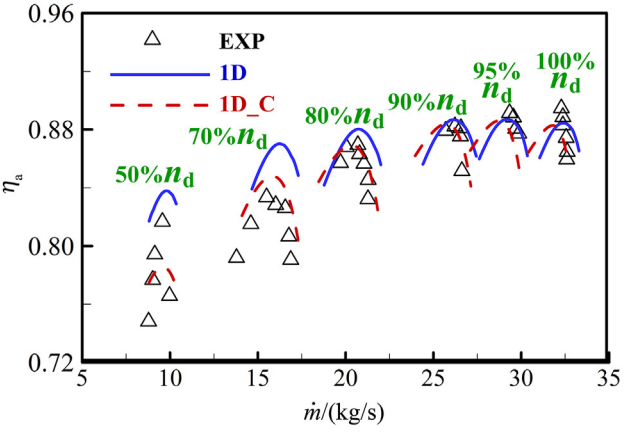

(b) Adiabatic efficiency

Figure 5 Overall performance of the P&WA compressor.

4. Re-stagger optimization and discussion

For the re-stagger optimization of the P&WA axial compressor, single-speed and multi-speed conditions are considered, and both involve multiple working points calculations. It should be mentioned that the centrifugal part of the P&WA compressor is not modeled, but flow angle matching issue is considered in the optimization.

4.1. Single-speed re-stagger optimization (SSOpt)

4.1.1. Design parameters and objective functions

The single-speed re-stagger optimization (SSOpt) means that optimization is conducted under a specific revolution. The objective is to maximize both the efficiency and surge margin. As noted in Ref. [25] and implied by Figure 5, the P&WA compressor has poor performance at speed of 70% n_d. Therefore, this speed condition is selected for the SSOpt. The operating point which has the maximum efficiency under this speed is regarded as the constrained point (CP). This means that the total pressure ratio (π_t) of the CP should be unchanged during the optimization, while the efficiency (η_a) of the CP is maximized.

Since π_t of the CP is not altered after optimization, the essence of the SSOpt is to rotate the characteristic curves around the CP. Figure 6 shows the feasible and unfeasible directions of this rotation. Compared to the original characteristic curve, i.e., C_{ori}, surge margin will be broadened if the C_{ori} curve revolves to the C_{fea} curve, while it will be narrowed if the C_{ori} curve revolves to the C_{unf} curve. Since variation of surge mass flow is small, optimization direction is significantly affected by the estimation accuracy of surge boundary models. So a multi-point optimization strategy is integrated into SSOpt, and SM is avoided in objective function, instead the efficiency at a near-stall point (SP) is optimized. The mathematical expression of the SSOpt problem is formulated as below:

$$\begin{aligned}
&\text{minimize } f_1(\chi) = \text{abs}\left(\pi_{t,opt,c} - \pi_{t,ori,c}\right)\\
&\text{minimize } f_2(\chi) = \left(1.0 - \eta_{a,opt,c}\right) + \left(1.0 - \eta_{a,opt,s}\right)\\
&\text{s.t.}\begin{cases} g_1(\chi) = \left(\pi_{t,opt,s} - \pi_{t,ori,s}\right) > 0.0 \\ g_2(\chi) = \left(D_{F,opt,c} - 0.60\right) < 0.0 \\ g_3(\chi) = \left(D_{F,opt,s} - 0.60\right) < 0.0 \end{cases}
\end{aligned} \tag{1}$$

where subscripts ori and opt are the original and optimized values, c and s stand for the constrained point and near-surge point respectively. In addition, D_F demonstrates blade diffusion factor. It is introduced to avoid results with unreasonable aerodynamic conditions.

Equality constraints in Eq. (1) can decrease the stability of the optimization and lead to local optimal solution. Due to this, the condition that π_t is unchanged is converted to an objective function, as indicated by $f_1(\chi)$ in Eq. (1). Moreover, the requirement of not altering π_t may reduce the feasible solution space during initial random sampling. In order to alleviate the issue, the revolution speed is added as an additional design variable. Since performance parameters at constrained and surge points are equally important, $f_2(\chi)$ is a weighted sum of the efficiency at these two conditions. The subtractive expression $(1-\eta_a)$ is to make $f_2(\chi)$ be minimized. The design variables for the SSOpt are stagger angles of the IGV and SVs, also the revolution.

4.1.2. SSOpt results

Using the SSOpt approach described above, two re-stagger arrangements are conducted. The first one optimizes stagger angles of IGV, S1 and S2 (IGV-S2), while the second optimizes those of IGV and S1−S5 (IGV-S5). For the second scheme, the stagger angle of S6 is fixed in order to guarantee the inlet flow angle of the subsequent centrifugal compressor. The optimization process is carried out for 70 generations, with 600 individuals for each generation. Results of both two SSOpt arrangements are shown in Figure 7, where Pareto fronts can be clearly identified. Since π_t is regarded as the primal criterion for selecting the feasible solution, so points with minimum values of $f_1(\chi)$ are chosen as the optimal solution, as indicated by SSOpt_IGV-S2 and SSOpt_IGV-S5 in Figure 7.

Detailed re-stagger information of the SSOpt_IGV-S2 and SSOpt_IGV-S5 are listed in Table 3. Values of γ are gradually decreased from the upstream IGV to downstream S5 at the nominal 70%n_d. It can also be seen from Table 3 that the SSOpt_IGV-S5 arrangement is more appropriate for multi-stage compressor. This is due to a fact that the front stages are easily surged while the rear stages are to be choked at part speed. The IGV, S1−S2 are closed and S3−S5 are opened in the SSOpt_IGV-S5 scheme. This is

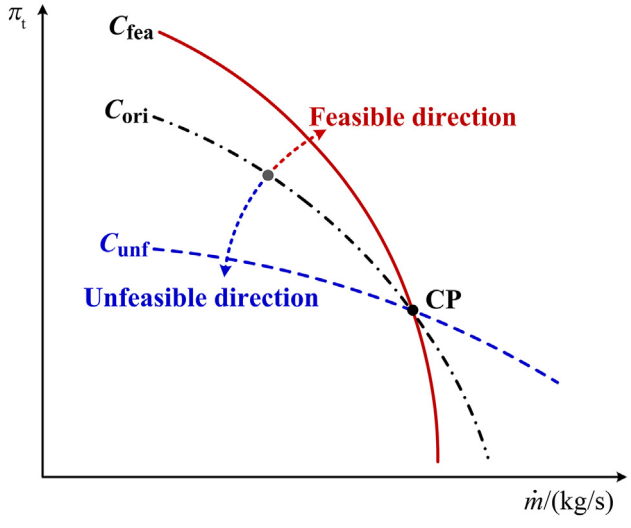

Figure 6 Illustration of optimization direction on one speed line.

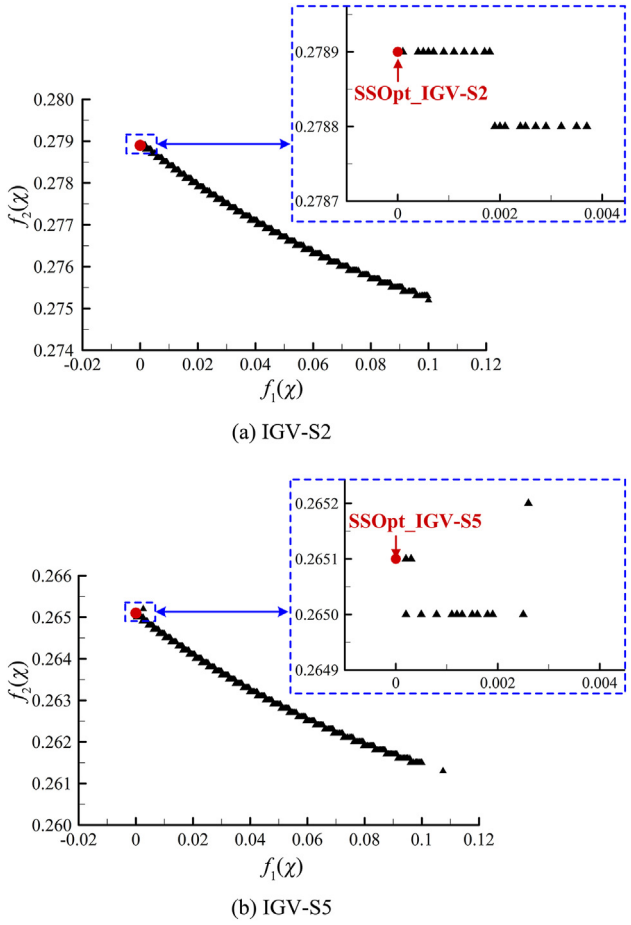

(a) IGV-S2

(b) IGV-S5

Figure 7 Objectives of the SSOpt.

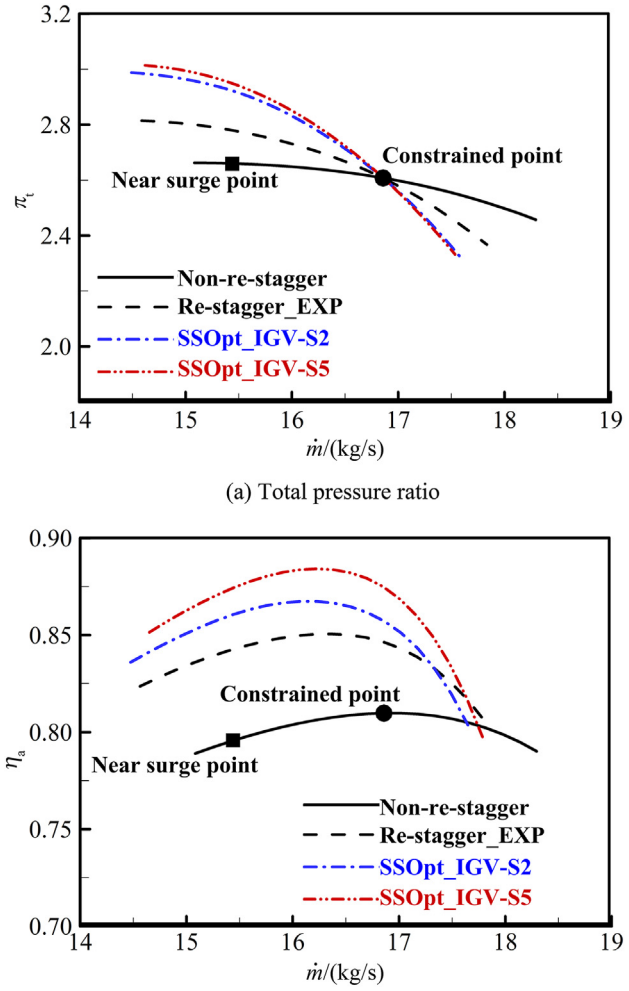

(a) Total pressure ratio

(b) Adiabatic efficiency

Figure 8 Comparison of characteristic curves for the P&WA 6-stage axial compressor at 70%n_d.

Table 3 Re-stagger schemes of the SSOpt.

	SSopt_IGV-S2	SSOpt_IGV-S5
n_{opt}/rpm	11062.8	10951.2
γ_{IGV}/(°)	40.000	39.999
γ_{S1}/(°)	14.998	14.998
γ_{S2}/(°)	10.000	10.000
γ_{S3}/(°)	–	0.361
γ_{S4}/(°)	–	−5.000
γ_{S5}/(°)	–	−4.933

beneficial to avoid the surge condition in front stages and to alleviate choke condition in rear stages.

Figure 8 plots the characteristic curves of the P&WA axial compressor at the nominal speed of 70%n_d. Non-re-stagger indicates performance data without re-stagger scheme, while re-stagger_EXP represents those with experimental re-stagger scheme [25]. All data are predicted using the 1D mean-line solver. It can be clearly seen that relative to the non-re-stagger curve, the experimental and both two optimized performance curves are revolved in clockwise around the constrained point. This is consistent with the analysis described in Figure 6. In order to evaluate the operating range, the SM is defined as:

$$\mathrm{SM} = \left(\frac{\pi_{t,s}}{\pi_{t,ori}}\frac{m_{ori}}{m_s} - 1\right) \times 100\% \tag{2}$$

It is found that compared to the non-re-stagger scheme, SSOpt_IGV-S2 and SSOpt_IGV-S5 improve the SM by 19.146% and 19.155% respectively, and increase with maximum efficiency by 6.015% and 6.805% respectively.

Figure 9 presents incidences (i) and off-design loss (ω) of blade rows from R1 to S6 at the CP. Both i and ω are calculated using empirical loss models. It can be observed that the re-stagger optimization rematches the blade rows to keep the incidences away from the stall ones, this is the reason why the surge margin and efficiency are increased at part speed in Figure 8. Although Figures 8 and 9 prove that the IGV-S5 optimization results are slightly better than those of IGV-S2, the structural cost and influence of vane end gaps can be significantly increased in this scheme. Therefore, the IGV-S2 results may be a more reasonable solution, which is consistent

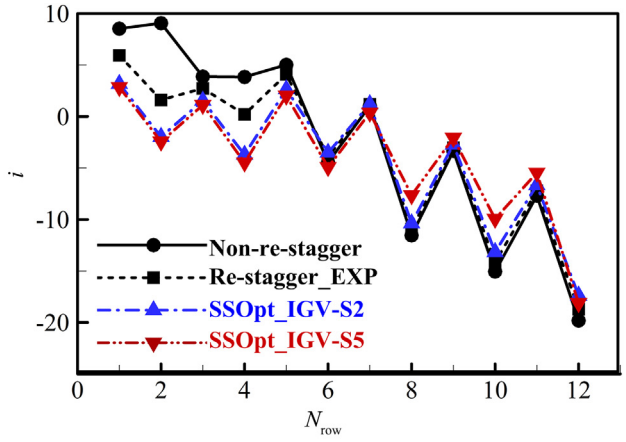

(a) Incidence

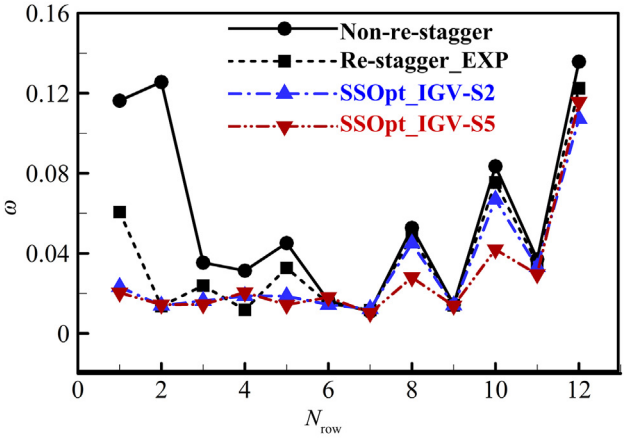

(b) Off-design loss

Figure 9 Incidences of blade rows at the operating point.

with the experimental scheme. All results verify that the re-stagger optimization can effectively identify re-stagger direction of variable vanes in preliminary design phase of compressors.

4.2. Multi-speed re-stagger optimization (MSOpt)

4.2.1. Design parameters and objective functions

The last section just considers one single-speed during the re-stagger optimization. In order to further improve the ability of VIGV&VSV for performance enhancement, multi-speed re-stagger optimization (MSOpt) is conducted for the PW&A 6-stage axial compressor. Four speed conditions are considered in MSOpt, and they are 70%n_d, 80% n_d, 90%n_d and 95%n_d respectively. Unlike the requirements in SSOpt, pressure ratio in MSOpt is not constrained, so the multi-point strategy in Section 4.1 is not adopted, and only the peak efficiency ($\eta_{a,max}$) of each speed condition is evaluated. Meanwhile, surge mass flow rate ($\dot{m}_s$) is to be minimized. The mathematical expressions of optimization can be written as:

$$\begin{aligned}
&\text{minimize } f_1(\chi) = \sum\left(\frac{\dot{m}_s - \dot{m}_{ref}}{\dot{m}_s}\right),\ i=1,2,3,4\\
&\text{minimize } f_2(\chi) = \sum(1.0 - \eta_{a,i,max}),\ i=1,2,3,4\\
&\text{s.t.}\begin{cases} g_1(\chi) = \dfrac{\Delta\gamma_{IGV,i} - \Delta\gamma_{IGV,100\%}}{n_i - n_d} - K_{IGV} = 0.0\\ g_2(\chi) = \Delta\gamma_{SV,i} - K_{SV}\Delta\gamma_{IGV,i} = 0.0 \end{cases}
\end{aligned} \tag{3}$$

where the subscript i represents each speed condition. Similar to the definition of $f_2(\chi)$ in Eq. (1), both $f_1(\chi)$ and $f_2(\chi)$ in Eq. (3) are weighted sum objective functions of the performance at the four speed conditions. For the function $f_1(\chi)$, $\dot{m}_{ref}$ is a reference mass flow, and $\dot{m}_s$ is predicted using the surge model. The subtractive formula in $f_2(\chi)$ is also to solve a minimization problem.

The two constraint functions in Eq. (3) are defined considering VSV controlling laws. For $g_1(\chi)$, a constant parameter is introduced to specify a linear relationship between the re-stagger angle and the revolution speed. This is due to a situation that γ is proportionally altered with n. The parameter K_{IGV} is a linear factor of experimental re-stagger schedules for IGV only. In addition, under multi-speed circumstances, a common rod is installed to simultaneously control the re-stagger setting of IGV and SVs to reduce complexity, weight, and cost of the structure [10]. This single-rod arrangement has been utilized in the LM2500 compressor [27], GE-E^3 compressor [28] and KHI 14-stage compressor [29]. Therefore, the second constraint function, $g_2(\chi)$, imposes a linear constraint for the variations in γ between IGV and stators, as implied by the factor K_{SV}. This setting is not same to the strategy in the SSOpt, where re-stagger angles of IGV and SVs are independently adjusted by separate mechanical structures. To summarize this section, it is easy to verify that there are 3 design variables for the MSOpt, namely $\Delta\gamma_{IGV,100\%}$, K_{IGV} and K_{SV}.

4.2.2. MSOpt results

For the MSOpt, two optimization arrangements are also considered. They are based on the re-stagger of IGV-S2 and IGV-S5, as termed as MSOpt_IGV-S2 and MSOpt_IGV-S5 respectively. During the MSOpt process, 70 generations and 200 populations are set respectively. Results show that for the MSOpt_IGV-S2 case, the convergence trend of $f_1(\chi)$ is the same as that of $f_2(\chi)$, so the Pareto-optimal front is converged to a point. For the MSOpt_IGV-S5 case, the Pareto front is shown in Figure 10. An optimal point is selected to realize the maximum efficiency, as shown by the red circle in the Figure 10.

The optimized re-stagger angles at various speed conditions are shown in Figure 11, while comparisons in performance are presented in Figure 12. Similar to the SSOpt, changing trend in γ from IGV to S2 designed by both two MSOpt cases is the same as that arranged in

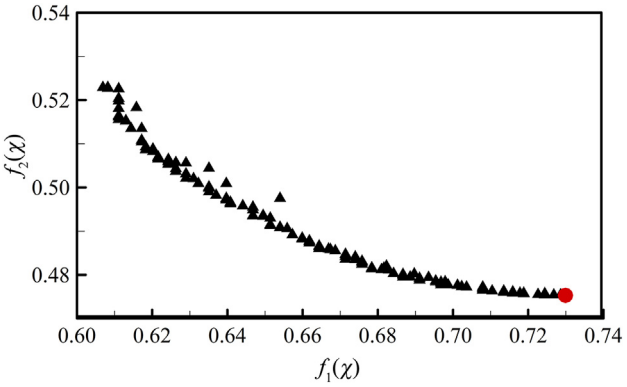

Figure 10 Objectives of the MSOpt_IGV-S5.

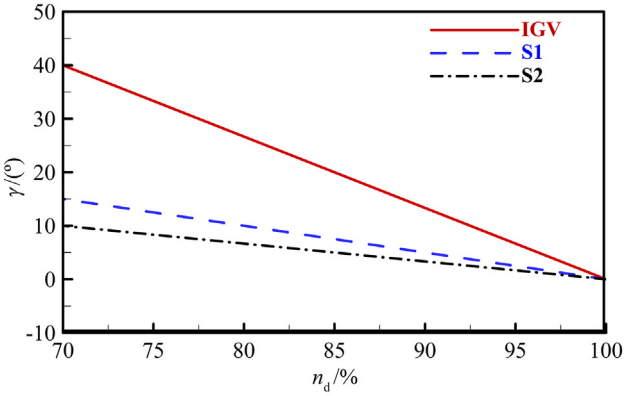

(a) MSOpt_IGV-S2

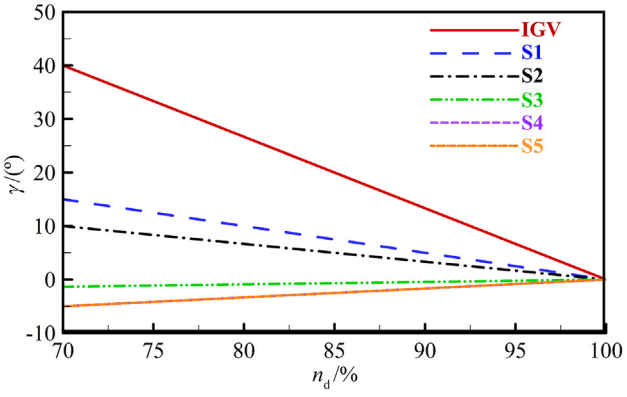

(b) MSOpt_IGV-S5

Figure 11 Re-stagger schedules obtained by the MSOpt.

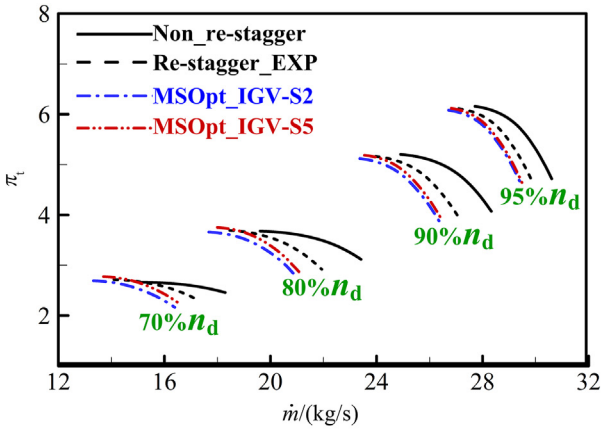

(a) Total pressure ratio

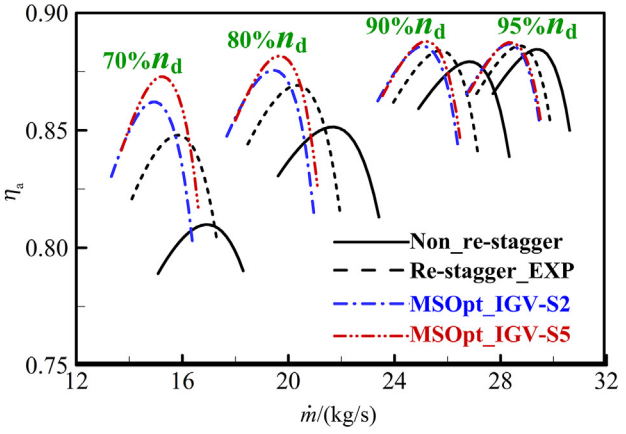

(b) Adiabatic efficiency

Figure 12 Characteristic curves of the P&WA 6-stage compressor after the MSOpt.

experiments. The re-stagger tendency of the MSOpt_IGV-S5 also reflects the part-speed operating features of multi-stage compressors, i.e., alleviating stall in front stages and choking in rear stages. In addition, Figure 12 demonstrates that both MSOpt schedules have smaller surge mass flow rate, larger efficiency, and wider surge margin than the experimental re-stagger settings. Compared with the MSOpt_IGV-S2 scheme, the MSOpt_IGV-S5 improves the performance only by a small extent. The maximum difference in peak efficiency between the two optimized schemes is 1.071% at 70%n_d. It implies that re-stagger the rear stages has a relatively small effect on performance improvement. This phenomenon is also observed in many compressors [27–29]. All results illustrate the effectiveness of the developed re-stagger optimization schedule.

It is noticed that results of the MSOpt at 70%n_d is basically the same as that of the SSOpt, and the optimal setting is achieved at bounds set by Table 2. This indicates that the performance at 70%n_d dominates the multi-speed optimization, also serves as a validation of each other. The adjustable ranges are set by real structures, which also limit the achieved performance. Also, the obtained re-stagger setting is different with that of the experiment (shown in Figure 4). This is may due to that the experimental setting is not aimed at aerodynamic performance only, or is the result of a comprise between VSV, bleeding and/or matching with the centrifugal compressor stage. However, the predicted effects, as shown in Figures 8 and 12, verify the correctness of both the experiment and optimization results in the present study.

4.3. Method of locating a working point for a specific pressure ratio or mass flow rate

It can be seen from Figures 8 and 12 that the characteristic curves are obviously altered after the re-stagger optimization. Therefore, it is necessary to determine reasonable working points to get required off-design performance for the re-staggered compressor. Due to this, a method to ascertain the working point under a certain pressure ratio is proposed. The re-stagger scheme illustrated in Figure 4 is used here, and the pressure ratio is fixed to be 4.18. Corresponding characteristic curves are shown in Figure 13.

There are many operating points that can achieve the required π_t, e.g., P1, P2 and P3 in Figure 13. For these points, mass flow rates are increased with enlarging the revolution speed. Meanwhile, the adiabatic efficiency is first increased and then decreased with raising the mass flow rate, see Figure 14. This corresponds to the condition changing from stall to the choke, so the working point is determined according to the maximum efficiency, as demonstrated by P4.

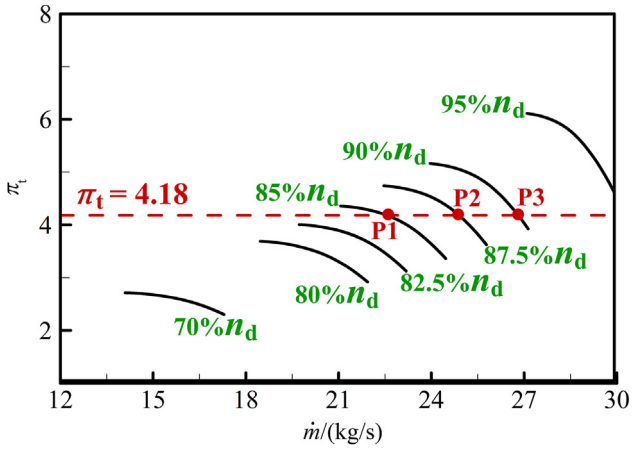

Figure 13 Schematic diagram of characteristic curves when VIGV/VSV used.

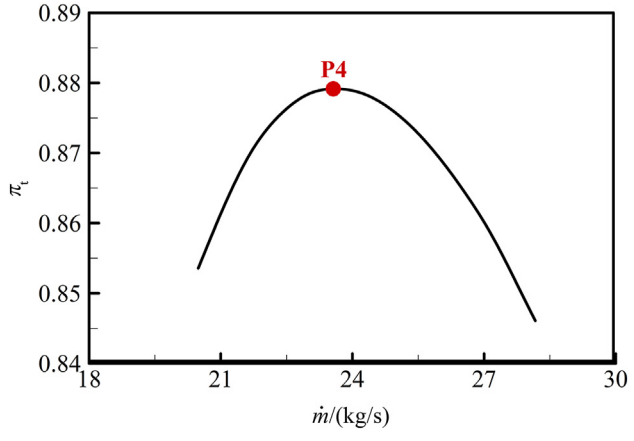

Figure 14 Relationship between mass flow rate and efficiency with a specified total pressure ratio when VIGV/VSV used.

In order to get the working point which can realize the maximum efficiency for the specific π_t, an optimization using the genetic algorithm is conducted. The revolution speed is regarded as the design parameter. Results indicate when the efficiency reaches to the maximum value, the revolution speed and the mass flow rate are 86.1%n_d and 23.696 kg/s respectively. This is nearly consistent with the point P4 in Figure 14. Therefore, this method can be utilized to determine working points for other pressure ratios to get a reasonable operating line.

The same philosophy can also be applied when a mass flow rate, instead of total pressure ratio, is specified. Those procedures may be used in the matching axial compressors with other components.

5. Conclusions

A re-stagger optimization method for variable stator vanes is proposed in this paper to improve off-design aerodynamic performance of multistage axial compressors. It integrates a mean-line performance analysis method and the multi-objective NSGA-II optimization algorithm. Prediction accuracy of the mean-line analysis method is improved via integrating a model calibration procedure. Two common applications, namely single-speed and multiple-speed re-stagger optimizations, are carried out for a multistage axial compressor with VIGV and VSV. Stagger angles of rows from IGV to second stage stator (IGV-S2), and from IGV to five-stage stator (IGV-S5) are optimized.

In the single-speed optimization, mass flow rate and pressure ratio of the operating point are constrained, and "multi-point" processing is employed to guide the optimization direction. Results show that compared with the fixed geometry, the IGV-S2 scheme can improve the surge margin and maximum efficiency by 19.146% and 6.015% respectively. In addition, optimized surge margin and efficiency of IGV-S5 approach are only 0.008% and 0.790% higher than those of IGV-S2 scheme. For the multi-speed optimization, off-design performance of the compressor with re-staggered vanes is significantly improved, and performance improvements of the IGV-S5 scheme is also small when compared with the IGV-S2.

Moreover, the tendency of re-stagger schemes obtained by both single-speed and multi-speed optimizations is consistent with those of experimental test. But the optimized schemes have higher efficiency and wider surge margin. A final achievement of this paper is that a screening method is established to identify the operating point of a compressor with variable geometry under a user-defined pressure ratio or mass flow rate.

In summary, the above results demonstrate effectiveness and stability of the re-stagger optimization method. This method is based on 1D performance solver, so it can be easily combined with other techniques to determine a more comprehensive and reasonable active control scheme for compressors in engineering applications.

Acknowledgements

The authors would like to thank the National Natural Science Foundation of China (Grant No.51606026) for funding this work.

References

[1] R.H. Aungier, Axial-Flow Compressors, ASME Press, New York, 2003.
[2] J.J. Sun, R.L. Elder, Numerical optimization of a stator vane setting in multistage axial-flow compressors, Proc. Inst. Mech. Eng. Part A: J. Power Energy 212 (4) (1998) 247−259.
[3] L. Gallar, M. Arias, V. Pachidis, R. Singh, Stochastic axial compressor variable geometry schedule optimisation, Aero. Sci. Technol. 15 (5) (2011) 366−374.
[4] D.B. Alone, S.S. Kumar, S.M. Thimmaiah, J.R.R. Mudipalli, A.M. Pradeep, S. Ramamurthy, V.S. Iyengar, Stability management of high speed axial flow compressor stage through axial extensions of bend skewed casing treatment, Propul. Power Res. 5 (3) (2016) 236−249.
[5] Q.G. Zheng, H.B. Zhang, Z.F. Ye, L.Z. Miao, Acceleration process optimization control of turbofan engine based on variable guide vane adjustment, J. Aero. Power 31 (11) (2016) 2801−2808.
[6] H. Chang, W.G. Zhao, D.H. Jin, Z.Y. Peng, X.M. Gui, Numerical investigation of base-setting of stator's stagger angles for a 15-stage axial-flow compressor, J. Therm. Sci. 23 (1) (2014) 36−44.
[7] L. Shi, B. Liu, P. Zhang, J. Li, L. Wang, One-dimensional characteristic optimization design for ten-stage high pressure compressor in commercial engine, J. Aero. Power 28 (7) (2013) 1564−1569.
[8] H. Roh, S. Daley, The online optimisation of stator vane settings in multi-stage axial compressors, Int. J. Adv. Mechatron. Syst. (IJAMechS) 1 (4) (2009) 266−279.
[9] N.M. White, A. Tourlidakis, R.L. Elder, Axial compressor performance modelling with a quasi-one-dimensional approach, Proc. Inst. Mech. Eng. Part A: J. Power Energy 216 (2) (2002) 181−193.
[10] L. Gallar, M. Arias, V. Pachidis, P. Pilidis, Compressor variable geometry schedule optimisation using genetic algorithms, in: Proceedings of ASME Turbo Expo: Power for Land, Sea, and Air, Orlando, Florida, USA, June 8-12, Paper No. GT2009-60049, 2009.
[11] S. Reitenbach, M. Schnoes, R.G. Becker, T. Otten, Optimization of compressor variable geometry settings using multi-fidelity simulation, in: Proceedings of ASME Turbo Expo: Power for Land, Sea, and Air, Montreal, Quebec, Canada, June 15−19, Paper No. GT2015-42832, 2015.
[12] Z.T. Wang, J. Li, K. Fan, S.Y. Li, The off-design performance simulation of marine gas turbine based on optimum scheduling of variable stator vanes, Math. Probl Eng. (2007) Article ID 2671251.
[13] B. Li, C.W. Gu, X.T. Li, T.Q. Liu, Numerical optimization for stator vane settings of multi-stage compressors based on neural networks and genetic algorithms, Aero. Sci. Technol. 52 (2016) 81−94.
[14] R.O. Bullock, I.A. Johnsen, Aerodynamic design of axial flow compressors, National Aeronautics and Space Administration Report, No. NASA-SP-36, 1965.
[15] A.D.S. Carter, H.P. Hughes, A Theoretical Investigation into the Effect of Profile Shape on the Performance of Aerofoils in Cascade, Aeronautical Research Council Reports and Memoranda, No. 2384, 1946.
[16] C.C. Koch, L.H. Smith, Loss sources and magnitudes in axial-flow compressors, J. Eng. Power 98 (3) (1976) 411−424.
[17] W.C. Moffatt, W. Jansen, The off-design analysis of axial-flow compressors, J. Eng. Power 89 (4) (1967) 453−462.
[18] H.F. Creveling, R.H. Carmody, Computer Program for Calculating Off-Design Performance of Multistage Axial-Flow Compressors, National Aeronautics and Space Administration Report, No. CR-72427, 1968.
[19] W.R. Davis, A Computer Program for the Analysis and Design of Turbomachinery-Revision, Carleton University, Revised Edition, Ottawa, 1971.
[20] C.C. Koch, Stalling pressure rise capability of axial flow compressor stages, J. Eng. Power 103 (4) (1981) 645−656.
[21] C. Peng, One-dimensional Performance Modeling and Variable Geometry Optimization of Multistage Axial Compressor, Master thesis, Dalian University of Technology, Dalian, Liaoning, 2019.
[22] M. Cetin, C. Hirsch, G.K. Serovy, Application of Modified Loss and Deviation Correlations to Transonic Axial Compressors, Advisory Group for Aerospace Research and Development Report, No. AGARD-R-745, 1987.
[23] T. Rowan, Functional Stability Analysis of Numerical Algorithms, Ph.D. thesis, University of Texas at Austin, Austin, 1990.
[24] K. Deb, A. Pratap, S. Agarwal, T. Meyarivan, A fast and elitist multiobjective genetic algorithm: NSGA-II, IEEE Trans. Evol. Comput. 6 (2) (2002) 182−197.
[25] J.K. Schweitzer, B.T. Brown, Advanced Industrial Gas Turbine Technology Readiness Demonstration Program: Final Report, Phase I: Design Study, USA Department of Energy Report No. HCP/T 5035, 1977.
[26] J.K. Schweitzer, J.D. Smith, Advanced Industrial Gas Turbine Technology Readiness Demonstration Program: Phase II Final Report: Compressor Rig Fabrication Assembly and Test, USA Department of Energy Report No. DOE/OR/05035-T2, 1981.
[27] A.R. Wadia, D.P. Wolf, F.G. Haaser, Aerodynamic design and testing of an axial flow compressor with pressure ratio of 23.3:1 for the LM2500+ gas turbine, J. Eng. Power 124 (3) (2002) 331−340.
[28] S.J. Cline, W. Fesler, H.S. Liu, R.C. Lovell, S.J. Shaffer, High Pressure Compressor Component Performance Report, National Aeronautics and Space Administration Report, No. NASA-CR-168245, 1983.
[29] T. Ikeguchi, A. Matsuoka, Y. Sakai, Y. Sakano, K. Yoshiura, Design and development of a 14-stage axial compressor for industrial gas turbine, in: Proceedings of ASME Turbo Expo: Power for Land, Sea, and Air, Copenhagen, Denmark, June 11-15, Paper No. GT2012-68524, 2012.